

1 **Editor Decision: Publish subject to minor revisions (further review by Editor)** (04 Sep
2 2017) by Christian Stamm

3 Comments to the Author:

4 Dear Dr. Song

5

6 Thanks for your Revision. There a just two technical details:

7

8 My comment to L. 1624: I was probably not clear want I exptected. You mentioned in
9 your first response that you provide the regressions for Fig. 3 etc. without points that
10 can be considered outliers. I had these metrics in mind. It would be nice to add a table
11 in the SI listing These regressions (including R², p values) and refering to that table in
12 the figure captions.

13

14 **Response:** the authors thank you for the concern and detailed suggestion, we did the
15 regressions without these high DOC values, which is preferentially regarded as outliers,
16 and all the regression metrics (i.e., coefficient of determination (R²), slope, intercept
17 and p-value) were provided in Table S6. Further, the main text was changed
18 correspondingly with respect to the supplementary Table S6. We really thank you for
19 the kind suggestion.

20

21 L. 328 in the latest Version: I suggest to correct to "... CDOM essentially originates
22 from ...".

23 **Response:** we thank you for the correction of the grammatical problem, and your kind
24 suggestion was incorporated in the revised manuscript.

25

26 Upon these modifications I can accept the manuscript.

27

28 Sincerely

29

30 Christian Stamm

31

32

33

A systematic examination of the relationships between CDOM and DOC in inland waters in China

Kaishan Song¹, Ying Zhao^{1, 2}, Zhidan Wen¹, Chong Fang^{1, 2}, Yingxin Shang¹

¹Northeast Institute of Geography and Agroecology, CAS, Changchun, 130102, China

² University of Chinese Academy of Sciences, Beijing 100049, China

Corresponding author's E-mail: songks@iga.ac.cn; Tel: 86-431-85542364

40

41 **Abstract:** Chromophoric dissolved organic matter (CDOM) plays a vital role in the
42 biogeochemical cycle in aquatic ecosystems. The relationship between CDOM and
43 dissolved organic carbon (DOC) has been investigated, and the significant relationship
44 lays the foundation for the estimation of DOC using remotely sensed imagery data. The
45 current study examined the samples from freshwater lakes, saline lakes, rivers and
46 streams, urban water bodies, and ice-covered lakes in China for tracking the variation
47 of the relationships between DOC and CDOM. The regression model slopes for DOC
48 versus $a_{CDOM}(275)$ ranged from extreme low 0.33 (highly saline lakes) to 1.03 (urban
49 waters) and 3.01 (river waters). The low values were observed in saline lake waters and
50 waters from semi-arid or arid regions where strong photo-bleaching is expected due to
51 less cloud cover, longer water residence time and daylight hours. In contrast, high
52 values were found in waters developed in wetlands or forest in Northeast China, where
53 more organic matter was transported from catchment to waters. The study also
54 demonstrated that closer relationships between CDOM and DOC were revealed when
55 $a_{CDOM}(275)$ were sorted by the ratio of $a_{CDOM}(250)/a_{CDOM}(365)$, which is a measure for

56 the CDOM absorption with respect to its composition, and the determination of
57 coefficient of the regression models ranged from 0.79 to 0.98 for different groups of
58 waters. Our results indicated the relationships between CDOM and DOC are variable
59 for different inland waters, thus models for DOC estimation through linking with
60 CDOM absorption need to be tailored according to water types.

61

62 **Keywords:** Absorption, CDOM, DOC, regression slope, saline water, fresh water

63

64 **1. Introduction**

65 Inland waters play a disproportional role for the global carbon cycling with respect to
66 carbon transportation, transformation and carbon storage (Tranvik et al., 2009;
67 Raymond et al., 2013; Verpoorter et al., 2014; Yang et al., 2015). However, the amount
68 of dissolved organic carbon (DOC) stored in the inland waters is still unclear or the
69 uncertainty is still needed to be evaluated (Tranvik et al., 2009). Determination DOC
70 concentration is straightforward through field sampling and laboratory analysis
71 (Findlay and Sinsabaugh, 2003). However, there are millions of lakes in the world, and
72 many of them are remote and inaccessible, making it impossible to evaluate DOC
73 concentration using routine approach (Cardille et al., 2013; Brezonik et al., 2015; Pekel
74 et al., 2016). Researchers have found that remote sensing might provide a promising
75 tool for quantification of DOC of inland waters at large scale through linking DOC with
76 chromophoric dissolved organic matter (CDOM), particularly for inland waters
77 situating in remote area with less accessibility (Tranvik et al., 2009; Kutser et al., 2015;
78 Brezonik et al., 2015).

79 As one of the optically active constituents (OACs) in waters, CDOM can be
80 estimated through remotely sensed signals (Yu et al., 2010; Kutser et al., 2015), and is
81 acted as a proxy in many regions for the amount of DOC in the water column. As shown
82 in Fig.1, CDOM and DOC in the aquatic ecosystems are mainly originated from natural
83 external (allochthonous) and internal (autochthonous) sources, in addition to directly
84 discharge from anthropogenic activities (Zhou et al., 2016). Generally, the
85 autochthonous CDOM ~~is~~—essentially originates from algae and macrophytes, and

86 mainly consists of various compounds of low molecular weights (Findlay and
87 Sinsabaugh, 2003; Zhang et al., 2010). While, the allochthonous CDOM is mainly
88 derived from the surrounding terrestrial ecosystems, and it comprises a continuum of
89 small organic molecules to highly polymeric humic substances. In terms of CDOM
90 originating from anthropogenic sources, it contains fatty acid, amino acid and sugar,
91 thus the composition of CDOM is more complex than that from natural systems (Zhou
92 et al., 2016; Zhao et al., 2016a). Hydrological factors also affect the DOC and CDOM
93 characteristic and particularly, the discharge, catchment area, land use and travel time
94 are the important ones (Neff et al., 2006; Spencer et al., 2012).

95 **[Insert Fig.1 about here]**

96 CDOM is a light-absorbing constituent, which is partially responsible for the color
97 in waters (Bricaud et al., 1981; Reche et al., 1999; Babin et al., 2003). The chemical
98 structure and origin of CDOM can be characterized by its absorption coefficients
99 ($a_{CDOM}(\lambda)$) and spectral slopes (De Haan and De Boer, 1987; Helms et al., 2008).
100 Weishaar et al. (2003) has proven that the carbon specific absorption coefficient at 254
101 nm, e.g., SUVA₂₅₄ is a good tracer for the aromaticity of humic acid in CDOM, while
102 the ratio of CDOM absorption at 250 to 365 nm, i.e., $a_{CDOM}(250)/a_{CDOM}(365)$, herein,
103 M value, has been successfully used to track the variation in DOM molecular weight
104 (De Haan and De Boer, 1987). Biodegradation and photodegradation are the major
105 processes to determine the transformation and composition of CDOM (Findlay and
106 Sinsabaugh, 2003; Zhang et al., 2010), which ultimately affect the relationship between
107 DOC and CDOM (Spencer et al., 2012; Yu et al., 2016). With prolonged sunlight

108 radiation, some of the colored fraction of CDOM is lost by the photobleaching
109 processes (Miller et al., 1995; Zhang et al., 2010), which can be measured by the light
110 absorbance decreasing at some specific (diagnostic) wavelength, e.g., 250, 254, 275,
111 295, 360 and 440 nm.

112 It should be noted that $a_{CDOM}(440)$ is usually used by remote sensing community
113 due to this wavelength is overlapped with pigment absorption at 443 nm, thus reporting
114 $a_{CDOM}(440)$ has potential to improve chlorophyll-a estimation accuracy (Lee et al.,
115 2002). The relationship between CDOM and DOC varies since CDOM loses color while
116 the variation of DOC concentration is almost negligible. Saline or brackish lakes in the
117 arid or semi-arid regions are generally exposed to longer sunlight radiation, thus CDOM
118 absorbance decreases, while DOC is accumulated due to the longer residence time
119 (Curtis and Adams, 1995; Song et al., 2013; Wen et al., 2016). Compared to
120 photodegradation of CDOM, the biodegradation processes by microbes are much more
121 complicated, and extracellular enzymes are the key factors required to decompose the
122 high-molecular-weight CDOM into low-molecular-weight substrates (Findlay and
123 Sinsabaugh, 2003). With compositional change, the absorption feature of CDOM and
124 its relation to DOC varies correspondingly, and the relationship between CDOM and
125 DOC needs to be systematically examined (Gonnelli et al., 2013). In addition, the
126 SUVA₂₅₄ and M value may be used to classify CDOM into different groups and enhance
127 the relationship with DOC based on CDOM absorption grouping.

128 Some studies have investigated the spatial and seasonal variations of CDOM and
129 DOC in ice free season in lakes, rivers and oceans (Vodacek et al., 1997; Neff et al.,

130 2006; Stedmon et al., 2011; Brezonik et al., 2015), but less is known about saline lakes
131 (Song et al., 2013; Wen et al., 2016). Even less is known about urban waters influenced
132 by sewage effluent and waters with ice cover in winter (Belzile et al., 2002; Zhao et al.,
133 2016b). A significant relationship between CDOM and DOC was observed in the Gulf
134 of Mexico, and stable regression model was established between DOC and a_{CDOM} (275)
135 and a_{CDOM} (295) (Fichot and Benner, 2011). Similar results were also found in other
136 estuaries along a salinity gradient, for example the Baltic Sea surface water (Kowalczuk
137 et al., 2010) and the Chesapeake Bay (Le et al., 2013). However, Chen et al. (2004)
138 found that the relationship between CDOM and DOC was not conservative due to
139 estuarine mixing or photo-degradation. Similar arguments were raised for Congo River
140 and waters across mainland USA (Spencer et al., 2009, 2012). In addition, seasonal
141 variations were observed in some studies due to the mixing of various endmembers of
142 CDOM from different terrestrial ecosystems and internal source (Zhang et al., 2010;
143 Spencer et al., 2012; Yu et al., 2016; Zhou et al., 2016).

144 As demonstrated in Fig.1, several factors influence the association between DOC
145 and CDOM, thus the relationship between DOC and CDOM may vary with respect to
146 their origins, photo- or bio-degradations, and hydrological features, which is worth of
147 systematic examination. In this study, the characteristics of DOC and CDOM in
148 different inland waters across China were examined to determine the spatial feature
149 associated with landscape variations, hydrologic conditions and saline gradients. The
150 objectives of this study are to: 1) examine the relationship between CDOM and DOC
151 concentrations across a wide range of waters with various physical, chemical and

152 biological conditions, and 2) develop a model for the relationship between DOC and
153 CDOM based on the sorted CDOM absorption feature, e.g., the M values with aiming
154 to improve the regression modeling accuracy.

155 **2. Materials and Methods**

156 The dataset is composed of five subsets of samples collected from various types of
157 waters across China (Table 1, Fig.2), which encompassed a wide range of DOC and
158 CDOM. The first dataset (n = 288; from early spring 2009 to late October 2014)
159 includes samples collected in freshwater lakes and reservoirs during the growing season
160 with various landscape types. The second dataset (n = 345; from early spring 2010 to
161 late mid-September 2014) includes samples collected in brackish to saline water bodies.
162 The third dataset (n = 322; from early May 2012 to late July 2015) includes samples
163 collected in rivers and streams across different basins in China. In addition, 69 samples
164 were collected from three sections along the Songhua River, the Yalu and the Hunjiang
165 River during the ice free period in 2015 to examine the impact of river flow on the
166 relationship between DOC and CDOM (see Fig.S1 for location). The fourth dataset (n
167 = 328; from 2011 to 2014 in the ice frozen season) includes samples collected in
168 Northeast China in winter from both lake ice and underlying waters. The fifth dataset
169 (n = 221; from early May 2013 to mid-October 2014) collects samples in urban water
170 bodies, including lakes, ponds, rivers and streams, which were severely polluted by
171 sewage effluents. City maps and Landsat imagery data acquired in 2014 or 2015 were
172 used to delineate urban boundaries with ArcGIS 10.0 (ESRI Inc., Redlands, California,
173 USA), and water bodies in these investigated cities constrained by urban boundaries

174 were considered as urban water bodies. The sampling dates, water body names and
175 locations of other types of water bodies were provided in supplementary Table S1-4.

176 [Insert Fig.2 about here]

177 **2.1 Water quality determination**

178 Water samples were collected approximately 0.5m below the water surface at each
179 station, generally locating in the middle of water bodies. Water samples were collected
180 in two 1 L amber HDPE bottles, and kept in coolers with ice packs in the field and kept
181 in refrigerator at 4°C after shipping back to the laboratory. All samples were
182 preprocessed (e.g., filtration, pH and electrical conductivity (EC) determination) within
183 two days in the laboratory. Water salinity was measured using DDS-307 EC meter
184 ($\mu\text{S}/\text{cm}$) at room temperature ($20\pm2^\circ\text{C}$) in the laboratory and converted to *in situ* salinity,
185 expressed in practical salinity units (PSU). Water samples were filtered using Whatman
186 cellulose acetone filter with pore size of 0.45 μm . Chlorophyll-a (Chl-a) was extracted
187 and concentration was measured using a Shimadzu UV-2600PC spectrophotometer, the
188 details can be found in Jeffrey and Humphrey (1975). Total suspended matter (TSM)
189 was determined gravimetrically using pre-combusted Whatman GF/F filters with
190 0.7 μm pore size, details can be found in Song et al. (2013). DOC concentrations were
191 measured by high temperature combustion (HTC) with water samples filtered through
192 0.45 μm Whatman cellulose acetone filters (Zhao et al., 2016a). The standards for
193 dissolved total carbon (DTC) were prepared from reagent grade potassium hydrogen
194 phthalate in ultra-pure water, while dissolved inorganic carbon (DIC) were determined
195 using a mixture of anhydrous sodium carbonate and sodium hydrogen carbonate. DOC

196 was calculated by subtracting DIC from DTC, both of which were measured using a
197 Total Organic Carbon Analyzer (TOC-VCPN, Shimadzu, Japan). Total nitrogen (TN)
198 was measured based on the absorption levels at 146 nm of water samples decomposed
199 with alkaline potassium peroxydisulfate. Total phosphorus (TP) was determined using
200 the molybdenum blue method after the samples were digested with potassium
201 peroxydisulfate (APHA, 1998). pH was measured using a PHS-3C pH meter at room
202 temperature (20±2°C).

203 **2.2 CDOM absorption measurement**

204 All water samples were filtered at low pressure at two steps: 1) filtered at low pressure
205 through a pre-combusted Whatman GF/F filter (0.7µm), and 2) further filtered through
206 pre-rinsed 25 mm Millipore membrane cellulose filter (0.22 µm). Absorption spectra
207 were obtained between 200 and 800 nm at 1 nm increment using a Shimadzu UV-
208 2600PC UV-Vis dual beam spectrophotometer (Shimadzu Inc., Japan) through a 1 cm
209 quartz cuvette (or 5 cm cuvette for ice melted water samples). Milli-Q water was used
210 as reference for CDOM absorption measurements. The Napierian absorption coefficient
211 (a_{CDOM}) was calculated from the measured optical density (OD) of samples using Eq.
212 (1):

$$213 \quad a_{CDOM}(\lambda) = 2.303[OD_{S(\lambda)} - OD_{(null)}] / \beta \quad (1)$$

214 where β is the cuvette path length (0.01 or 0.05m) and 2.303 is the conversion factor of
215 base 10 to base e logarithms. To remove the scattering effect from the limited fine
216 particles remained in the filtered solutions, a necessitated correction was implemented
217 by assuming the average optical density over 740–750 nm to be zero (Babin et al., 2003).

218 SUVA₂₅₄ and M values were calculated to characterize CDOM with respect to their
219 compositional features. In addition, a_{CDOM} was divided into different groups according
220 to M values by hierarchical cluster approach, which was performed in SPSS software
221 package with the pairwise distance between samples was measured by squared
222 Euclidean distance and the clusters were linked together by Ward's linkage method
223 (Ward Jr, 1963). The method has been applied to classify the waters into different types
224 according the remote sensing spectra (Vantrepotte et al., 2012; Shi et al., 2013).

225 **3. Results**

226 **3.1. Water quality characteristics**

227 Chl-a concentrations ($46.44 \pm 59.71 \mu\text{g/L}$) ranged from 0.28 to $521.12 \mu\text{g/L}$. TN and TP
228 concentrations were very high in fresh lakes, saline lakes and particularly urban water
229 bodies (Table 1). It is worth noting that Chl-a concentration was still high 7.3 ± 19.7
230 $\mu\text{g/L}$ even in ice-covered lakes in winter from Northeast China. Electric conductivity
231 (EC) and pH were high in the semi-arid and arid regions, and they were 1067-41000
232 $\mu\text{s/cm}$ and 7.1-11.4, respectively. Overall, waters were highly turbid with high TSM
233 concentrations ($119.6 \pm 131.4 \text{ mg/L}$), and apparent variations were observed for
234 different types of waters (Table 1). Hydrographic conditions exerted strong impact on
235 water turbidity and TSM concentration, thus these two parameters of river and stream
236 samples were excluded in this study (Table 1).

237 **[Insert Table 1 about here]**

238 **3.2. DOC concentrations in different types of waters**

239 DOC concentrations changed remarkably in the investigated waters (Table 1). The

240 concentration of DOC were low in rivers, and the lowest DOC concentrations were
241 measured in ice melting waters. It should be noted that large variations were observed
242 in water samples from rivers and streams (Table 2). Among the five types of waters,
243 relatively higher DOC concentrations, ranging from 2.3 to 300.6 mg/L, were found in
244 many saline lakes, in the Songnen Plain, the Hulunbuir Plateau and some areas in
245 Tibetan Plateau (see Fig.2 for location). However, some of saline lakes supplied by
246 snow melt water or ground water exhibited relatively lower DOC concentrations even
247 with high salinity. Compared with samples collected in growing seasons, higher DOC
248 concentrations (7.3-720 mg/L) were observed in ice-covered water bodies.

249 [Insert Table 2 about here]

250 **3.3. DOC versus CDOM for various types of waters**

251 ***3.3.1 Freshwater lakes and reservoirs***

252 The relationship between DOC and CDOM has been investigated based on CDOM
253 absorption at different wavelengths (Fichot and Benner, 2011; Spencer et al., 2012;
254 Song et al., 2013; Brezonik et al., 2015). As suggested by Fichot and Benner (2011),
255 CDOM absorptions at 275 nm ($a_{CDOM}(275)$) and 295 nm ($a_{CDOM}(295)$) have stable
256 performances for DOC estimates for coastal waters. In current study, a strong
257 relationship ($R^2 = 0.85$) between DOC and $a_{CDOM}(275)$ was found in fresh lakes and
258 reservoirs (Fig.3a). However, the inclusion of $a_{CDOM}(295)$ explains very limited
259 variance, thus it is not considered in the regression models. Regression analyses of
260 water samples collected from different regions indicated that the slopes varied from
261 1.30 to 3.01 (Table 3). Water samples collected from East China and South China had

262 lower regression slope values (Table 3), and lakes and reservoirs were generally
263 mesotrophic or eutrophic (Huang et al., 2014; Yang et al., 2012, and references therein).

264 [Insert Table 3 about here]

265 [Insert Fig.3 about here]

266 **3.3.2 Saline lakes**

267 A strong relationship between DOC and acDOM(275) ($R^2 = 0.85$) was demonstrated for
268 saline lakes (Fig.3b) with much lower regression slope value (slope = 1.28). Further,
269 the regression slopes exhibited large variations in different regions (Table 3), ranging
270 from 0.86 in Tibetan waters to 2.83 in the Songnen Plain waters (see Fig.2 for location).

271 As the extreme case, the slope value was only 0.33 as demonstrated in the embedded
272 diagram in Fig.3b. Saline lakes in semi-arid or arid regions generally exhibit higher
273 regression slope values, for example, the west Songnen Plain (2.83), the Hulunbir
274 Plateau and the East Inner Mongolia Plateau (1.79). Whereas, waters in the west Inner
275 Mongolia Plateau (1.13), the Tibetan Plateau (0.86) exhibited low slope values (Table
276 3), and the extreme low value was measured in the Lake Qinhai in Tibetan Plateau.

277 **3.3.3 Streams and rivers**

278 Although some of the samples scattered from the regression line (Fig.3c), close
279 relationship between DOC and acDOM(275) was found for samples collected in rivers
280 and streams. Compared with the other water types (Fig.3), rivers and streams exhibited
281 the highest regression slope value (slope = 3.01). Further regression analysis with water
282 samples sub-datasets collected in different regions indicated that slope values presented
283 large variability, ranging from 1.07 to 8.49. The lower regression slope values were

284 recorded in water samples collected in rivers and stream in semi-arid and arid regions,
285 such as the Tibetan Plateau, Mongolia Plateau and Tarim Basin, while the higher values
286 were found in samples collected in streams originated from wetland and forest in
287 Northeast China (Table 3).

288 To investigate the dynamics of CDOM absorption and DOC concentrations, three
289 sections were investigated in three major rivers in Northeast China (see Figure S1 for
290 location). River flow exerted obvious effect on DOC and CDOM (Fig.4) and flood
291 impulse brought large amount of DOC and CDOM into river channels. The
292 relationships between DOC and acDOM(275) in sections along three rivers in Northeast
293 China were demonstrated in Fig.5. The sampling point in the Yalu River is near the
294 river head source, thus strong relationship ($R^2=0.92$) was exhibited with large slope
295 (Fig.5a). The relationship between DOC and acDOM(275) in the Songhua River at
296 Harbin City section was much scattered ($R^2=0.64$, Fig.5c). With respect to Fig.5b, it is
297 an in-between case ($R^2=0.82$). The sampling point was affected by effluent from
298 Baishan City, thus the coefficient of determination ($R^2=0.822$) and the regression slope
299 (3.72) were lower than that from the Yalu River at Changbai point, while higher than
300 that from the Songhua River at Harbin point.

301 [Insert Fig.4 and Fig.5 about here]

302 **3.3.4 Urban waters**

303 As shown in Fig.3d, relatively close relationship between DOC and acDOM(275) was
304 revealed in urban waters ($R^2= 0.71$, $p<0.001$). Similarly, regression slope values for
305 urban waters also changed remarkably, ranging from 0.87 to 2.45 (Table 3). High

306 nutrients in urban waters (Table 1) usually result in algal bloom in most urban water
307 bodies (Chl-a range: 1.0-521.1 μ g/L; average: 38.9 μ g/L), which might contribute the
308 high DOC concentrations in urban waters (Table 1). Thereby, the contribution from
309 algal decomposition and cell lysis to DOC and CDOM should not be neglected for
310 urban waters (Zhang et al., 2010; Zhao et al., 2016b; Zhou et al., 2016).

311 ***3.3.5 Ice covered lakes and reservoirs***

312 The closest relationship ($R^2 = 0.93$) between DOC and $a_{CDOM}(275)$ was recorded in
313 waters beneath ice covered lakes and reservoirs in Northeast China (Fig.3e).
314 Comparatively, a weak relationship between DOC and $a_{CDOM}(275)$ was demonstrated
315 in ice melting waters (Fig.3f). Apparently, CDOM from ice melting waters were mainly
316 originated from maternal water during the ice formation, also from algal biological
317 processes (Stedmon et al., 2011; Arrigo et al., 2010). Interestingly, the regression slopes
318 for ice samples (1.35) and under lying water sample (1.27) are very close. In addition,
319 there was a significant relationship between DOC in ice and underlying waters ($R^2 =$
320 0.86), indicating the dominant components of CDOM and DOC in the ice are from
321 maternal underlying waters.

322 ***3.3.6 DOC versus $a_{CDOM}(440)$***

323 CDOM absorption at 440 nm, i.e., $a_{CDOM}(440)$, is usually used as a surrogate to
324 represent its concentration (Bricaud et al., 1981; Babin et al., 2003), and widely used in
325 remote sensing community to quantify CDOM in waters (Lee et al., 2002; Binding et
326 al., 2008; Zhu et al., 2014). Significant relationships between DOC and $a_{CDOM}(440)$
327 were found in different types of waters (Fig.5). Through comparing Fig.3 with Fig.6, it

328 can be found that the overall relationships between DOC and CDOM at 440 nm
329 resembled that at 275 nm for different types of waters, but with relatively loose
330 relationship as indicated by the coefficients of determination (see Table S5). Further, it
331 can be noted that some of the samples in Fig.3b-f and Fig.6b-f may leverage the
332 regression model performances. Thus, regression models without these samples
333 appearing to leverage the relationships were evaluated and provided in Table S6.
334 Comparing Table S5 and Table S6, the regression model performances were degraded,
335 but still acceptable.

336 [Insert Fig.6 about here]

337 **3.4 CDOM molecular weight and aromacity versus DOC**

338 ***3.4.1 CDOM versus SUVA₂₅₄ and M value (a_{CDOM}(250)/a_{CDOM}(365))***

339 The large slope variations of regressions between DOC and a_{CDOM}(275) in different
340 types of waters are probably due to the aromacity and colored fractions in DOC
341 component (Spencer et al., 2009, 2012; Lee et al., 2015). As shown in Fig.7a, it can be
342 seen that SUVA₂₅₄ had high values in fresh lakes, and waters from rivers or streams as
343 well. Saline water and ice covered waters in Northeast China showed intermediate
344 SUVA₂₅₄ values, while urban water and ice melting water exhibited lower values. The
345 M value, i.e., a_{CDOM}(250)/a_{CDOM}(365) is another indicator to demonstrate the variation
346 of molecular weight of CDOM components (De Haan, 1993). Compared to saline water,
347 fresh lake water (*t-Test*: F = 631, p < 0.01), river and stream water (*t-Test*: F = 565, p <
348 0.001), and urban water (*t-Test*: F = 393, p < 0.001) exhibited low M values (Fig.7b),
349 which indicated that large weight molecules dominate in these three types of waters.

350 Saline water, ice covered water in Northeast China and ice melting water showed higher
351 M values. Since SUVA₂₅₄ is a proxy based on the ratio to DOC, it is inappropriate to
352 establish the relationship between CDOM and DOC based on the SUVA₂₅₄
353 classification. Thereby, only M values, which reveal molecular weight and aromacity,
354 might help to estimate DOC through CDOM absorption based on M values for various
355 types of waters.

356 **[Insert Fig.7 about here]**

357 **3.4.2 Regression based on M values**

358 Regression models between DOC and a_{CDOM}(275) were established based on M value
359 grouping. Four groups were achieved with hierarchical cluster approach, and each
360 group occupied about 44.74% (M < 9.0), 34.24% (9.0 < M < 16.0), 18.22% (16.0 < M <
361 25.0) and 2.80% (25.0 < M < 68.0) of the total samples from group 1 to 4, respectively.
362 Though only M values were used in the cluster which meant the feature space in
363 classification only had one dimension and the groups were mainly divided according to
364 the distribution of M values, the hierarchical cluster approach generated rational results.
365 As shown in Fig.8, a close relationship ($R^2 = 0.90$) between DOC and a_{CDOM}(275) was
366 revealed in dataset where M < 9.0. Likewise, close relationship regression model
367 appeared in dataset with intermediate M values (Group 2 in Fig.8), revealing high
368 determination of coefficients ($R^2 = 0.91$). A relative weak relationship ($R^2 = 0.79$)
369 between DOC and a_{CDOM}(275) appeared with M values ranging from 16.0 to 25.0. A
370 very close relationship ($R^2 = 0.98$) was found with extremely high M values (Group 4
371 in Fig.8).

372 As noted in Fig.8, close regression slopes implicated that a comprehensive
373 regression model with intermediate M values less than 16 may be achieved. As
374 expected, a promising regression model (the diagram was not shown) between DOC
375 and $a_{CDOM}(275)$ was achieved ($y = 1.269x + 6.42$, $R^2 = 0.909$, $N = 1171$, $p < 0.001$) with
376 pooled dataset in group 1 and group 2 shown in Fig.8. Inspired by this idea, the
377 relationship between $a_{CDOM}(275)$ and DOC also examined with pooled data. As shown
378 in Fig.9a, a significant relationship between DOC and $a_{CDOM}(275)$ was obtained with
379 the pooled dataset ($N = 1504$) collected from different types of inland waters. However,
380 it should be noted that the extremely high DOC samples may advantageously contribute
381 the better performance of the regression model. Thus, regression model excluding these
382 eight samples ($DOC > 300$ mg/L) was acceptable (Fig.9b, $R^2 = 0.51$, $p < 0.001$), but
383 greatly degraded. In addition, regression model with power function was established in
384 decimal logarithms log-log scale (Fig.9c, $R^2 = 0.77$, $p < 0.001$).

385 [Insert Fig.8 and Fig.9 about here]

386 **4. Discussion**

387 **4.1 Variation of water quality parameters**

388 Different water types were sampled across China with different climatic, hydrologic,
389 and land use conditions in various catchment, combined with different anthropogenic
390 intensity, thus the biological and geochemical properties in the water bodies are quite
391 diverse with large range values for each parameters (Table 1). Extremely turbid waters
392 are observed for fresh waters, saline waters and underlying waters covered by ice,
393 which were generally collected in very shallow water bodies in different parts of China.

394 As expected, large variations of Chl-a are observed for both fresh waters and urban
395 waters, and particularly these samples collected in urban waters show large range (1.0-
396 521.1 μ g/L). Our investigation also indicates that algal growth is still very active in
397 these ice covered water bodies in Northeast China, which might result from high TN
398 (4.3 \pm 5.4mg/L) and TP (0.7 \pm 0.6mg/L) concentrations in these waters bodies. It also
399 should be noted that DOC, EC and pH were high in semi-arid or arid climatic regions,
400 which are consistent with previous findings (Curtis and Adams, 1995; Song et al., 2013;
401 Wen et al., 2016).

402 **4.2 DOC variation with different types of waters**

403 This investigation indicates that lower DOC were encountered with samples collected
404 in rivers from the Tibetan Plateau (Table 2), where the average soil organic matter is
405 lower, thus terrestrial DOC input from the catchment is less (Tian et al., 2008). However,
406 high DOC concentrations were found in rivers or streams surrounded by forest or
407 wetlands in Northeast China, the similar findings were also reported by Agren et al.
408 (2007, 2011). Further, lower DOC concentration is also measured with ice samples,
409 which is consistent with previous findings (Bezilie et al., 2002; Shao et al., 2016). But
410 relatively high DOC concentration was observed for underlying waters covered by ice
411 in Northeast China due to the condensed effect caused by the DOC discharged from ice
412 formation (Bezilie et al., 2002; Shao et al., 2016; Zhao et al., 2016a). This condensed
413 effect was particularly marked in these shallow water bodies where ice forming
414 remarkably condensed the DOC in the underlying waters (Zhao et al., 2016a). It also
415 should be noted that DOC concentration has a strong connection with hydrological

416 condition and catchment landscape features (Neff et al., 2006; Agren et al., 2007; Lee
417 et al., 2015). It should be noted that large DOC variations were observed in saline lakes
418 in different regions (Table 2). Much higher DOC concentrations were found in saline
419 lakes in Qinghai and Hulunbir, while relative low concentrations were observed in
420 Xilinguole Plateau and the Songnen Plain, which is consistent with previous
421 investigations conducted in the semi-arid or arid regions (Curtis and Adams, 1995;
422 Song et al., 2013; Wen et al., 2016).

423 **4.3 Variation of the relationships between CDOM and DOC**

424 As demonstrated in Fig.3, obvious variation is revealed for the regression slope values
425 between DOC and $a_{CDOM}(275)$. Most of the fresh water bodies are located in East China,
426 where agricultural pollution and anthropogenic discharge have resulted in serious
427 eutrophication (Tong et al., 2017). Phytoplankton degradation may contribute relative
428 large portion of CDOM and DOC in these water bodies (Zhang et al., 2010; Zhou et al.,
429 2016). Comparatively, fresh waters in Northeast and North China revealed larger
430 regression slopes (Table 3). Waters in Northeast China are surrounded by forest,
431 wetlands and grassland and therefore they generally exhibited high proportion of
432 colored fractions of DOC. Further, soils in Northeast China are rich in organic carbon,
433 which may also contribute to high concentration of DOC and CDOM in waters in this
434 region (Jin et al., 2016; Zhao et al., 2016a). Compared with waters in East and South
435 China, waters in Northeast China showed less algal bloom due to low temperature, thus
436 autochthonous CDOM was less presented in waters in Northeast China (Song et al.,
437 2013; Zhao et al., 2016a). As suggested by Brezonik et al. (2015) and Cardille et al.

438 (2013), CDOM in the eutrophic waters or those with very short resident time may show
439 seasonal variation due to algal bloom or hydrological variability, while CDOM in some
440 oligotrophic lakes or those with long resident time may show a stable pattern.

441 As shown in Fig.3b, smaller regression slope is revealed between DOC and
442 aCDOM(275) for saline waters, indicating less colored portion of DOC was presented in
443 waters in semi-arid to arid regions, especially for these closed lakes with enhanced
444 photochemical processes, enhanced by longer residence time and strong solar radiation
445 (Spencer et al., 2012; Song et al., 2013; Wen et al., 2016). The findings highlighted the
446 difference for the relationship between CDOM and DOC, thus different regression
447 models should be established to accurately estimate DOC in waters through linking
448 with CDOM absorption, particularly for fresh and saline waters that showing different
449 specific absorption coefficients (Song et al., 2013; Cardille et al., 2013; Brezonik et al.,
450 2015).

451 DOC concentration is strongly associated with hydrological conditions (Neff et al.
452 2006; Agren et al. 2007; Yu et al., 2016). The relationships between CDOM and DOC
453 in river and stream waters are very variable due to the hydrological variability and
454 catchment features (Agren et al., 2011; Spencer et al., 2012; Ward et al., 2013; Lee et
455 al., 2015; Zhao et al., 2017). As shown in Fig.4, the relationship between river flows
456 and DOC is rather complicated, which is mainly caused by the land use, soil properties,
457 relief, slope, the proportion of wetlands and forest, climate and hydrology of the
458 catchments (Neff et al., 2006; Sobek et al., 2007; Spencer et al., 2012; Zhou et al., 2016),
459 with additional influence by sewage discharge into rivers. The close relationship for

460 head waters with higher regression slope value (Fig.5a) is mainly attributed to that the
461 DOC and CDOM were fresh and less disturbed by pollution from anthropogenic
462 activities (Spencer et al., 2012; Shao et al., 2016). However, both point and non-point
463 source pollution complicated the relationship between DOC and DOM (Fig.5c).

464

465 **4.4 Regression models based on CDOM grouping**

466 As observed in Fig.3, the regression slopes (range: 0.33~3.01) for the relationship
467 between DOC and $a_{CDOM}(275)$ varied significantly. The CDOM absorption coefficient
468 is affected by its components and aromacity, thus the M values are used to classify
469 CDOM into different groups, which turns to be an effective approach for improving
470 regression models (Fig.8) between DOC and $a_{CDOM}(275)$. It also should be highlighted
471 that the fourth group (Fig.8) is mainly from saline lakes (samples from embedded
472 diagram in Fig.3b), thus the regression model slope is extremely low. From the
473 regression model with pooled data, it can also be seen that relative accurate regression
474 model for CDOM versus DOC can be achieved with data collected in inland waters at
475 global scale (Sobek et al., 2007), which might be helpful in quantifying DOC through
476 linking with CDOM absorption, and the latter parameter can be estimated from remote
477 sensing data (Zhu et al., 2011; Kuster et al., 2015). Comparing Fig.8 and Fig.9b, it also
478 should be noted that some of the saline waters with extremely low CDOM absorption
479 efficiency (Group 4 in Fig.8) should be divided into different groups to achieve accurate
480 DOC regression model through CDOM absorption.

481 **5. Conclusions**

482 Based on the measurement of CDOM absorption and DOC laboratory analysis, we have
483 systematically examined the relationships between CDOM and DOC in various types
484 of waters in China. This investigation showed that CDOM absorption varied
485 significantly. River waters and fresh lake waters exhibited high CDOM absorption
486 values and specific CDOM absorption ($SUVA_{254}$). On the contrast, saline lakes
487 illustrated low $SUVA_{254}$ values probably due to the long residence time and strong
488 photo-bleaching effects on waters in the semi-arid regions.

489 The current investigation indicated that the relationships between CDOM
490 absorption and DOC varied remarkably by showing very varied regression slopes in
491 various types of waters. Head river water generally exhibits larger regression slope
492 values, while rivers affected by anthropogenic activities show lower slope values.
493 Saline water generally reveals small regression slope due to the photobleaching effect
494 in the semi-arid or arid region, combined with longer residence time. The accuracy of
495 regression model between $a_{CDOM}(275)$ and DOC was improved when CDOM
496 absorptions were divided into different sub-groups according to M values. Our finding
497 highlights that remote sensing models for DOC estimation based on the relationship
498 between CDOM and DOC should consider water types or cluster waters into several
499 groups according to their absorption features.

500

501 **Acknowledgements**

502 The authors would like to thank financial supports from the National Key Research and
503 Development Project (No. 2016YFB0501502), Natural Science Foundation of China

504 (No.41471290 and 41730104), and “One Hundred Talents” Program from Chinese
505 Academy of Sciences granted to Dr. Kaishan Song. Thanks are also extended to all the
506 staff and students for their efforts in field data collection and laboratory analysis, and
507 Dr. Hong Yang to review and polish the English language. The authors are greatly
508 indebted to associate Editor C. Stamm and these referees from both the previous and
509 the current versions of the manuscript for their very valuable comments that greatly
510 strengthened this manuscript.

511

512 **References**

513 Agren, A., Buffam, I., Jansson, M., Laudon, H., 2007. Importance of seasonality and
514 small streams for the landscape regulation of dissolved organic carbon export.
515 Journal of Geophysical Research, 112: G03003.

516 Agren, A., Haei, M., Kohler, S.J., Kohler, S.J., Bishop, K., Laudon, H., 2011.
517 Regulation of stream water dissolved organic carbon (DOC) concentrations during
518 snowmelt; the role of discharge, winter climate and memory effects.
519 Biogeosciences, 7, 2901-2913.

520 APHA/AWWA/WEF. 1998. Standard methods for the examination of water and
521 wastewater. Washington, DC: American Public Health Association.

522 Arrigo, K.R., Mock, T., Lizotte, M.P., 2010. Primary producers and sea ice, In *Sea Ice*,
523 edited by D.N. Thomas, and G.S. Dieckmann, pp. 283-326, second ed., Wiley-
524 Blackwell, Oxford, UK.

525 Babin, M., Stramski, D., Ferrari, G. M., Claustre, H., Bricaud, A., Obolensky, G.,

526 Hoepffner, N., 2003. Variations in the light absorption coefficients of
527 phytoplankton, nonalgal particles, and dissolved organic matter in coastal waters
528 around Europe. *Journal of Geophysical Research*, 108(C7), 3211.

529 Belzile, C., Gibson, J.A.E., Vincent, W.F., 2002. Colored dissolved organic matter and
530 dissolved organic carbon exclusion from lake ice: implications for irradiance
531 transmission and carbon cycling. *Limnology and Oceanography*, 47(5), 1283–
532 1293.

533 Binding, C.E., Jerome, J.H., Bukata, R.P., Booty, W.G., 2008. Spectral absorption
534 properties of dissolved and particulate matter in Lake Erie. *Remote Sensing of
535 Environment*, 112(4), 1702-1711.

536 Brezonik, P.L., Olmanson, L.G., Finlay, J.C., Bauer, M.E., 2015. Factors affecting the
537 measurement of CDOM by remote sensing of optically complex inland waters.
538 *Remote Sensing of Environment*, 157, 199-215.

539 Bricaud, A., Morel, A., Prieur, L., 1981. Absorption by dissolved organic matter of the
540 sea (yellow substance) in the UV and visible domains, *Limnology and
541 Oceanography*, 26(1), 43– 53.

542 Cardille, J.A., Leguet, J.B., del Giorgio, P., 2013. Remote sensing of lake CDOM using
543 noncontemporaneous field data. *Canadian Journal of Remote Sensing*, 39, 118–
544 126.

545 Chen, R.F., Bissett, P., Coble, P., Conmy, R., Gardner, G.B., Moran, M.A., Wang, X.C.,
546 Wells, M.L., Whelan, P., Zepp, R.G., 2004. Chromophoric dissolved organic
547 matter (CDOM) source characterization in the Louisiana Bight. *Marine Chemistry*,

548 89, 257-272.

549 Curtis, P.J., Adams, H.E., 1995. Dissolved organic matter quantity and quality from
550 freshwater and saltwater lakes in east-central Alberta. *Biogeochemistry* 30, 59–
551 76.

552 De Haan, H., 1993. Solar UV-light penetration and photodegradation of humic
553 substances in peaty lake water. *Limnology and Oceanography*, 1993, 38, 1072–
554 1076.

555 De Haan, H., De Boer, T., 1987. Applicability of light absorbance and fluorescence as
556 measures of concentration and molecular size of dissolved organic carbon in
557 humic Lake Tjeukemeer. *Water Research*, 21, 731–734.

558 Fichot, C.G., Benner, R., 2011. A novel method to estimate DOC concentrations from
559 CDOM absorption coefficients in coastal waters. *Geophysical Research Letter*,
560 38, L03610.

561 Findlay, S.E.G., Sinsbaugh, R.L., 2003. *Aquatic Ecosystems Interactivity of Dissolved*
562 *Organic Matter*. Academic Press, San Diego, CA, USA.

563 Gonnelli, M., Vestri, S., Santinelli, C., 2013. Chromophoric dissolved organic matter
564 and microbial enzymatic activity. A biophysical approach to understand the marine
565 carbon cycle. *Biophysical Chemistry*, 182, 79-85.

566 Helms, J.R., Stubbins, A., Ritchie, J.D., Minor, E.C., Kieber, D.J., Mopper, K., 2008.
567 Absorption spectral slopes and slope ratios as indicators of molecular weight,
568 source, and photobleaching of chromophoric dissolved organic matter. *Limnology*
569 and *Oceanography*, 53, 955–969.

570 Huang, C.C., Li, Y.M., Yang, H., Li, J.S., Chen, X., Sun, D.Y., Le, C.F., Zou, J., Xu,
571 L.J., 2014. Assessment of water constituents in highly turbid productive water by
572 optimization bio-optical retrieval model after optical classification. *Journal of
573 Hydrology*, 519, 1572–1583.

574 Jaffé, R., McKnight, D., Maie, N., Cory, R., McDowell, W.H., Campbell, J.L., 2008.
575 Spatial and temporal variations in DOM composition in ecosystems: The
576 importance of long-term monitoring of optical properties. *Journal of Geophysical
577 Research*, 113, G04032.

578 Jeffrey, S.W., Humphrey G.F., 1975. New spectrophotometric equations for
579 determining chlorophylls *a*, *b*, *c₁*, and *c₂* in higher plants, algae and natural
580 phytoplankton. *Biochemie und Physiologie der Pflanzen*, 167(2), 191–194.

581 Jin, X.L., Du, J., Liu, H.J., Wang, Z.M., Song, K.S., 2016. Remote estimation of soil
582 organic matter content in the Sanjiang Plain, Northeast China: The optimal band
583 algorithm versus the GRA-ANN model. *Agricultural and Forest Meteorology*, 218,
584 250–260.

585 Kowalcuk, P., Zablocka, M., Sagan, S., Kulinski, K., 2010. Fluorescence measured in
586 situ as a proxy of CDOM absorption and DOC concentration in the Baltic Sea.
587 *Oceanologia*, 52(3), 431–471.

588 Kutser, T., Verpoorter, C., Paavel, B., Tranvik, L.J., 2015. Estimating lake carbon
589 fractions from remote sensing data. *Remote Sensing of Environment*, 157, 138–
590 146.

591 Lai, L., Huang, X., Yang, H., Chuai, X., Zhang, M., Zhong, T., Chen, Z., Chen, Y.,

592 Wang, X., Thompson, J.R., 2016. Carbon emissions from land-use change and
593 management in China between 1990 and 2010. *Science Advances*, 2(11),
594 e1601063.

595 Le, C.F., Hu, C.M., Cannizzaro, J., Duan, H.T., 2013. Long-term distribution patterns
596 of remotely sensed water quality parameters in Chesapeake Bay. *Estuarine,
597 Coastal and Shelf Science*, 128(10), 93–103.

598 Lee, E.J., Yoo, G.Y., Jeong, Y., Kim, K.U., Park, J.H., Oh, N.H., 2015. Comparison of
599 UV–VIS and FDOM sensors for in situ monitoring of stream DOC concentrations.
600 *Biogeosciences*, 12, 3109–3118.

601 Lee, Z.P., Carder, K.L., Arnone, R.A., 2002. Deriving inherent optical properties from
602 water color: A multiband quasi-analytical algorithm for optically deep waters.
603 *Applied Optics*, 41(27), 5755–577.

604 Miller, W.L., Zepp, R.G., 1995. Photochemical production of dissolved inorganic
605 carbon from terrestrial organic matter: Significance to the oceanic organic carbon
606 cycle. *Geophysical Research Letter*, 22 (4), 417–420.

607 Neff, J.C., Finlay, J.C., Zimov, S.A., Davydov, S.P., Carrasco, J.J., Schuur, E.A.G.,
608 Davydova, A.I., 2006. Seasonal changes in the age and structure of dissolved
609 organic carbon in Siberian rivers and streams. *Geophysical Research Letter*, 33,
610 L23401.

611 Pekel, J.F., Cottam, A., Gorelick, N., Belward, A.S., 2016. High-resolution mapping of
612 global surface water and its long-term changes. *Nature*, 540, 417–422.

613 Raymond, P. A., Hartmann, J., Lauerwald, R., et al., 2013. Global carbon dioxide

614 emissions from inland waters. *Nature*, 503(7476), 355–359.

615 Reche, I., Pace, M., Cole, J.J., 1999. Relationship of trophic and chemical conditions
616 to photobleaching of dissolved organic matter in lake ecosystems.
617 *Biogeochemistry*, 44, 529–280.

618 Shao, T.T., Song, K.S., Du, J., Zhao, Y., Ding, Z., Guan, Y., Liu, L., Zhang, B., 2016.
619 Seasonal variations of CDOM optical properties in rivers across the Liaohe Delta.
620 *Wetlands*, 36 (suppl.1): 181–192.

621 Shi, K., Li, Y., Li, L., et al., 2013. Remote chlorophyll-a estimates for inland waters
622 based on a cluster-based classification. *Science of the Total Environment*, 444, 1–
623 15.

624 Spencer, R.G.M., Stubbins, A., Hernes, P.J., Baker, A., Mopper, K., Aufdenkampe,
625 A.K., Dyda, R.Y., Mwamba, V.L., Mangangu, A.M., Wabakanghanzi, J.N., Six,
626 J., 2009. Photochemical degradation of dissolved organic matter and dissolved
627 ligninphenols from the Congo River. *Journal of Geophysical Research*, 114,
628 G03010.

629 Spencer, R.G.M., Butler, K.D., Aiken, G.R., 2012. Dissolved organic carbon and
630 chromophoric dissolved organic matter properties of rivers in the USA. *Journal*
631 *of Geophysical Research*, 117, G03001.

632 Sobek, S., Tranvik, L.J., Prairie, Y.T., Kortelainen, P., Cole, J.J., 2007. Patterns and
633 regulation of dissolved organic carbon: An analysis of 7,500 widely distributed
634 lakes. *Limnology and Oceanography* 52, 1208–1219.

635 Song, K.S., Zang, S.Y., Zhao, Y., Li, L., Du, J., Zhang, N.N., Wang, X.D., Shao, T.T.,

636 Liu, L., Guan, Y., 2013. Spatiotemporal characterization of dissolved Carbon for
637 inland waters in semi-humid/semiarid region, China. *Hydrology and Earth
638 System Science*, 17, 4269–4281.

639 Stedmon, C.A., Thomas, D.N., Papadimitriou, S., Granskog, M.A., Dieckmann, G.S.
640 2011. Using fluorescence to characterize dissolved organic matter in Antarctic
641 sea ice brines. *Journal of Geophysical Research*, 116, G03027.

642 Tian, Y.Q., Ouyang, H., Xu, X.L., Song, M.H., Zhou, C.P., 2008. Distribution
643 characteristics of soil organic carbon storage and density on the Qinghai-Tibet
644 Plateau. *Acta Pedologica Sinica*, 45(5), 933–942. (In Chinese with English
645 abstract).

646 Tong, Y.D., Zhang, W., Wang, X.J., et al., 2017. Decline in Chinese lake phosphorus
647 concentration accompanied by shift in sources since 2006. *Nature Geoscience*,
648 10(7), 507–511.

649 Tranvik, L.J., Downing, J.A., Cotner, J.B., et al., 2009. Lakes and reservoirs as
650 regulators of carbon cycling and climate. *Limnology and Oceanography*, 54(6),
651 2298–2314.

652 Vantrepotte, V., Loisel, H., Dessailly, D., et al., 2012. Optical classification of
653 contrasted coastal waters. *Remote Sensing of Environment*, 123, 306–323.

654 Verpoorter, C., Kutser, T., Seekell, D.A., Tranvik, L.J., 2014. A global inventory of
655 lakes based on high-resolution satellite imagery. *Geophysical Research Letter*, 41,
656 6396–6402.

657 Vodacek, A., Blough, N.V., Degrandpre, M.D., Peltzer, E.T., Nelson, R.K., 1997.

658 Seasonal variation of CDOM and DOC in the Middle Atlantic Bight: terrestrial
659 inputs and photooxidation. *Limnology and Oceanography*, 42, 674–686.

660 Ward Jr, J.H., 1963. Hierarchical grouping to optimize an objective function. *Journal of*
661 *the American Statistical Association*, 58(301), 236–244.

662 Ward, N.D., Keil, R.G., Medeiros, P.M., Brito, D.C., Cunha, A.C., Dittmar, T., Yager,
663 P.L., Krusche, A.V. and Richey, J.E., 2013. Degradation of terrestrially derived
664 macromolecules in the Amazon River. *Nature Geoscience*, 6(7), 530–533.

665 Weishaar, J.L., Aiken, G.R., Bergamaschi, B.A., Fram, M.S., Fugii, R., Mopper, K.,
666 2003. Evaluation of specific ultraviolet absorbance as an indicator of the chemical
667 composition and reactivity of dissolved organic carbon. *Environmental Science
668 and Technology*, 37, 4702–4708.

669 Wen, Z.D., Song, K.S., Zhao, Y., Du, J., Ma, J.H., 2016. Influence of environmental
670 factors on spectral characteristic of chromophoric dissolved organic matter
671 (CDOM) in Inner Mongolia Plateau, China. *Hydrology and Earth System
672 Sciences*, 20, 787–801.

673 Williamson, C.E., Rose, K.C., 2010. When UV meets fresh water. *Science*, 329, 637–
674 639.

675 Wilson, H., Xenopoulos, M.A., 2008. Ecosystem and seasonal control of stream
676 dissolved organic carbon along a gradient of land use. *Ecosystems* 11, 555–568.

677 Yang, H., Andersen, T., Dörsch, P., Tominaga, K., Thrane, J.-E., Hessen, D. O., 2015.
678 Greenhouse gas metabolism in Nordic boreal lakes. *Biogeochemistry*, 126, 211–
679 225.

680 Yang, H., Xie, P., Ni, L., Flower, R. J., 2012. Pollution in the Yangtze. *Science*, 337,
681 (6093), 410-410.

682 Yu, Q., Tian, Y. Q., Chen, R.F., Liu, A., Gardner, G.B., Zhu, W.N., 2010. Functional
683 linear analysis of in situ hyperspectral data for assessing CDOM in
684 rivers. *Photogrammetric Engineering & Remote Sensing*, 76(10), 1147–1158.

685 Yu, X.L., Shen, F., Liu, Y.Y., 2016. Light absorption properties of CDOM in the
686 Changjiang (Yangtze) estuarine and coastal waters: An alternative approach for
687 DOC estimation. *Estuarine, Coastal and Shelf Science*, 181, 302–311.

688 Zhang, Y.L., Zhang, E.L., Yin, Y., Van Dijk, M.A., Feng, L.Q., Shi, Z.Q., Liu, M.L.,
689 Qin, B.Q., 2010. Characteristics and sources of chromophoric dissolved organic
690 matter in lakes of the Yungui Plateau, China, differing in trophic state and altitude.
691 *Limnology and Oceanography*, 55(6), 2645–2659.

692 Zhao, Y., Song, K.S., Wen, Z.D., Li, L., Zang, S.Y., Shao, T.T., Li, S.J., Du, J., 2016a.
693 Seasonal characterization of CDOM for lakes in semiarid regions of Northeast
694 China using excitation–emission matrix fluorescence and parallel factor analysis
695 (EEM – PARAFAC). *Biogeosciences*, 13, 1635–1645.

696 Zhao, Y., Song, K.S., Li, S.J., Ma, J.H., Wen, Z.D., 2016b. Characterization of CDOM
697 from urban waters in Northern-Northeastern China using excitation–emission
698 matrix fluorescence and parallel factor analysis. *Environmental Science and
699 Pollution Research*, 23, 15381–15394.

700 Zhao, Y., Song, K.S., Shang, Y. X., Shao, T. T., Wen, Z.D., Lv, L.L., 2017.
701 Characterization of CDOM of river waters in China using fluorescence excitation–

702 emission matrix and regional integration techniques. *Journal of Geophysical*
703 *Research, Biogeoscience*, DOI: 10.1002/2017JG003820.

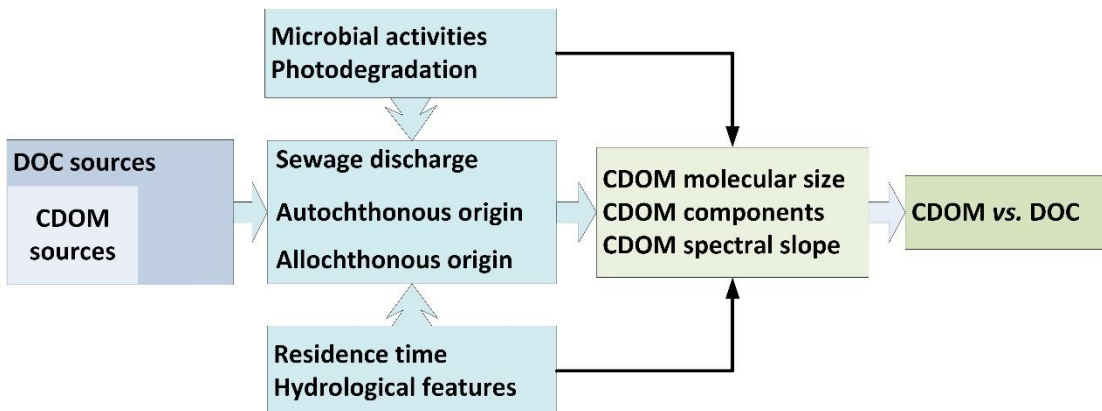
704 Zhou Y., Zhang Y., Jeppesen E., Murphy K.R., Shi K., Liu M., Liu X., Zhu G. Inflow
705 rate-driven changes in the composition and dynamics of chromophoric dissolved
706 organic matter in a large drinking water lake. *Water Research*, 2016, 100, 211-221.

707 Zhu, W., Yu, Q., Tian, Y. Q., Chen, R.F., Gardner, G.B., 2011. Estimation of
708 chromophoric dissolved organic matter in the Mississippi and Atchafalaya river
709 plume regions using above-surface hyperspectral remote sensing. *Journal of*
710 *Geophysical Research: Oceans (1978–2012)*, 116(C2), C02011.

711 Zhu, W.N., Yu, Q., Tian, Y. Q., et al., 2014. An assessment of remote sensing algorithms
712 for colored dissolved organic matter in complex freshwater environments. *Remote*
713 *Sensing of Environment*, 140, 766-778.

714 **Figures**

715 Fig.1. The potential regulating factors that influence the relationship between CDOM
716 and DOC. Note, CDOM sources are a subset of DOC sources, and hydrological feature
717 includes flow discharge, drainage area, catchment landscape, river level, and inflow or
718 outflow regions.



719

720

721

722

723

724

725

726

727

728

729

730

731

732

733

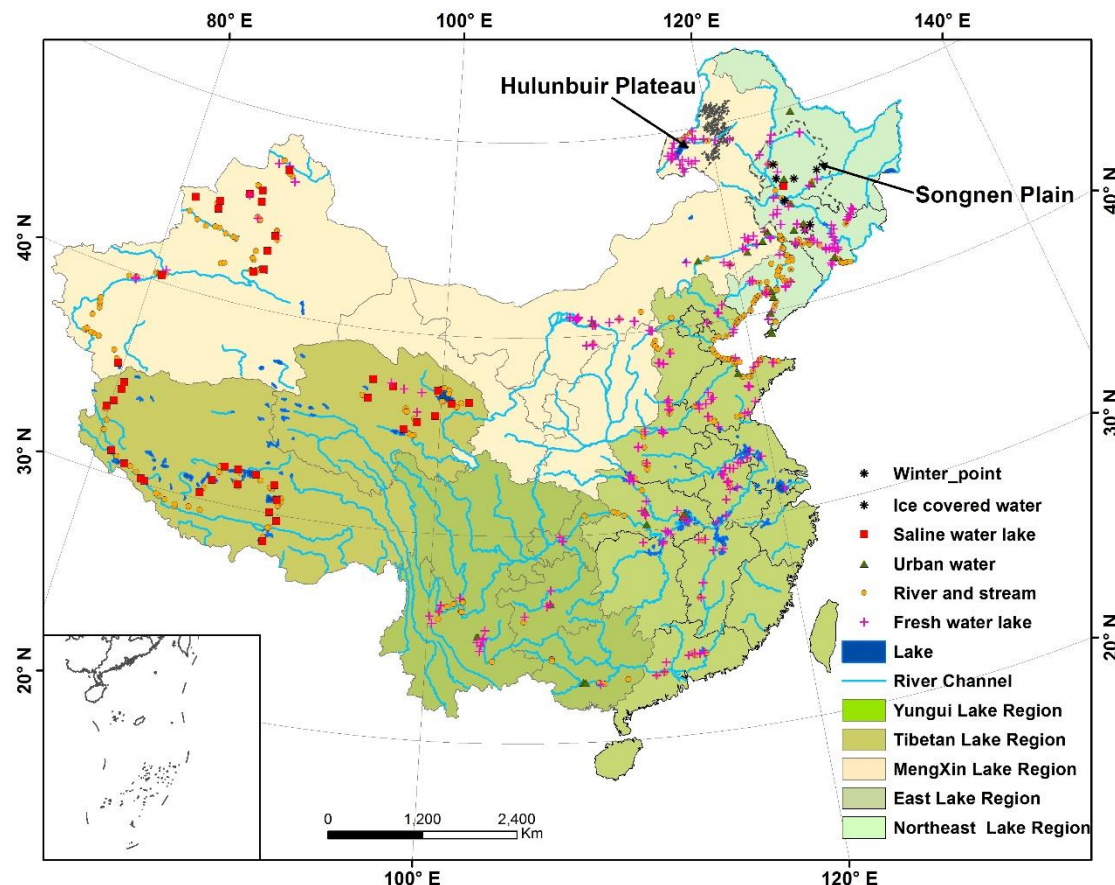
734

735

736

737

738 Fig.2. Water types and sample distributions across the mainland China. The dash line
739 shows the boundary of some typical geographic units (i.e., Songnen Plain, and
740 Hulunbuir Plateau).



741

742

743

744

745

746

747

748

749

750

751

752

753

754

755

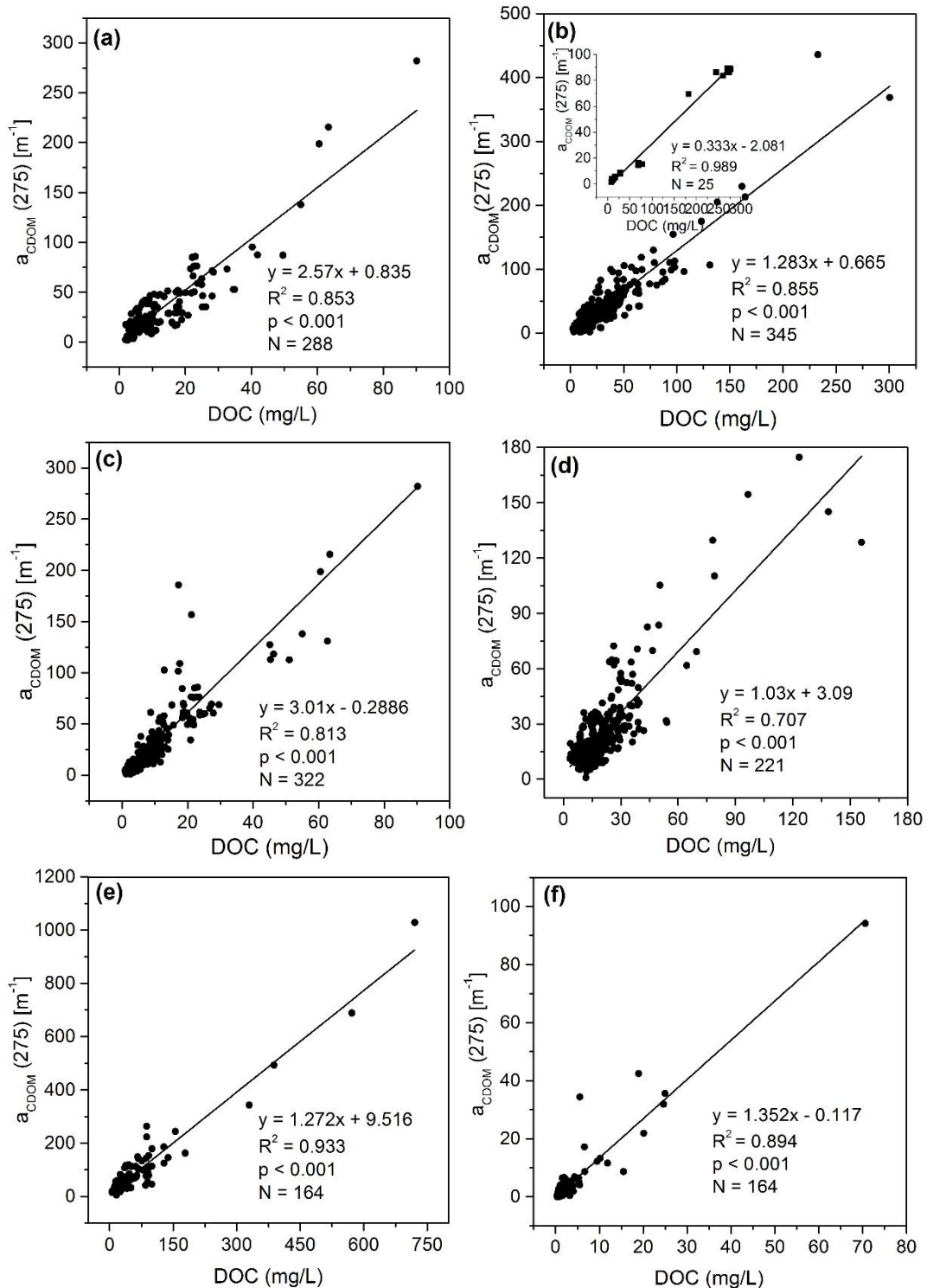
756

757

758

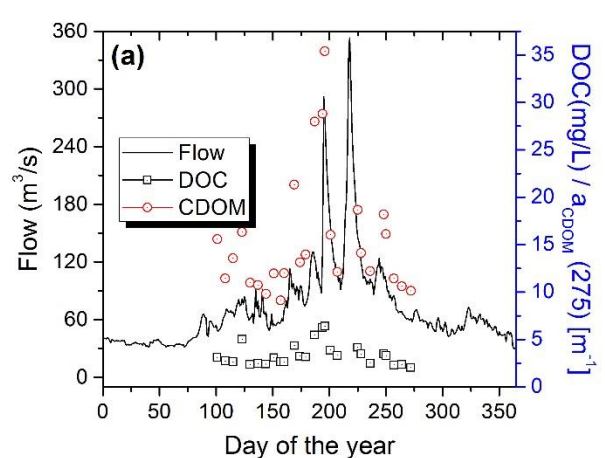
759

760 Fig.3. Relationship between DOC and $a_{CDOM}(275)$ in different types of inland waters,
 761 (a) fresh water lakes, (b) saline water lakes, (c) river and stream waters, (d) urban waters,
 762 (e) ice covered lake underlying waters, and (f) ice melting lake waters. The regression
 763 metrics without these high DOC concentrations in Fig.3b-f were listed in Tables S6.

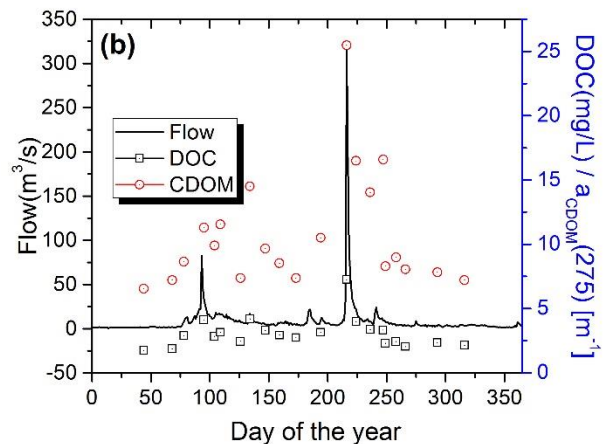


769 Fig.4. Concurrent flow dynamics for three rivers in Northeast China and the
 770 corresponding DOC and CDOM variations in 2015; (a) the Yalu River near Changbai
 771 County, (b) the Hunjiang River with DOC and CDOM sampled at Baishan City, while
 772 the river flow gauge station is near the Tonghua City, (c) the Songhua River at Harbin
 773 City.

774



775

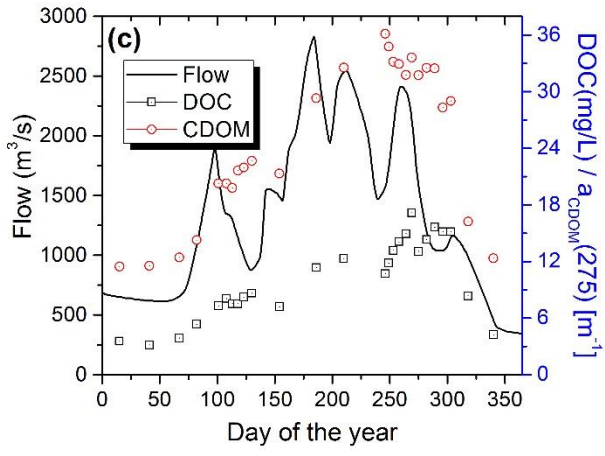


776

777

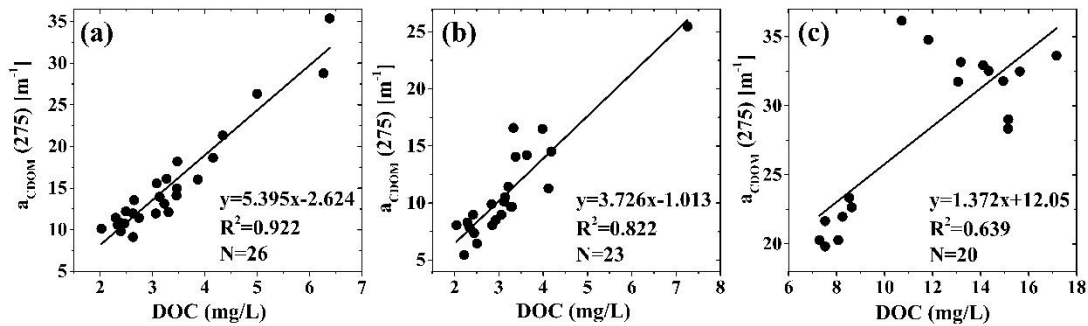
778

779



780 Fig.5. The relationships between aCDOM(275) and DOC at sections across (a) the Yalu
781 River, (b) the Hunjiang River, and (c) the Songhua River. The samples were collected
782 at each station at about one week or around ten days in ice free season in 2015.

783



784

785

786

787

788

789

790

791

792

793

794

795

796

797

798

799

800

801

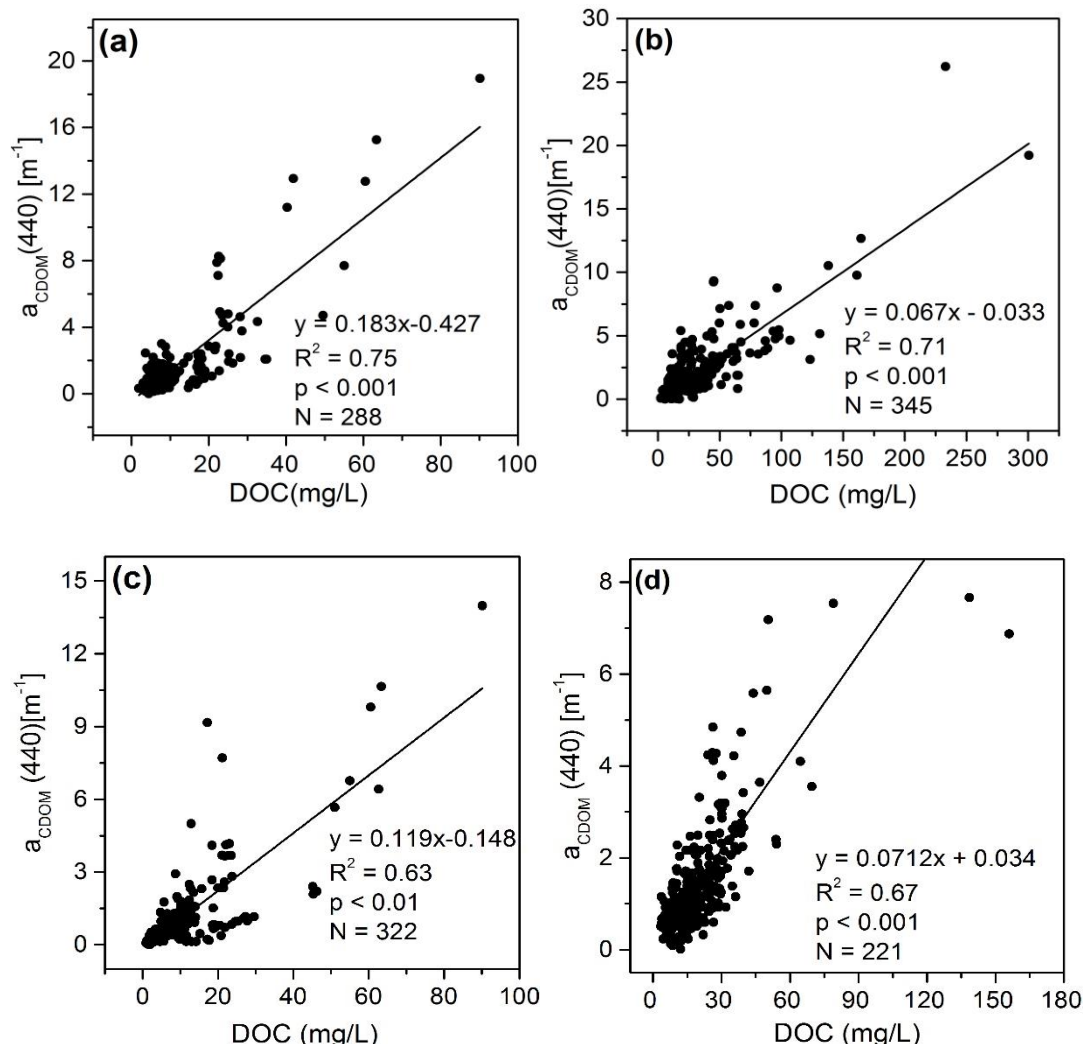
802

803

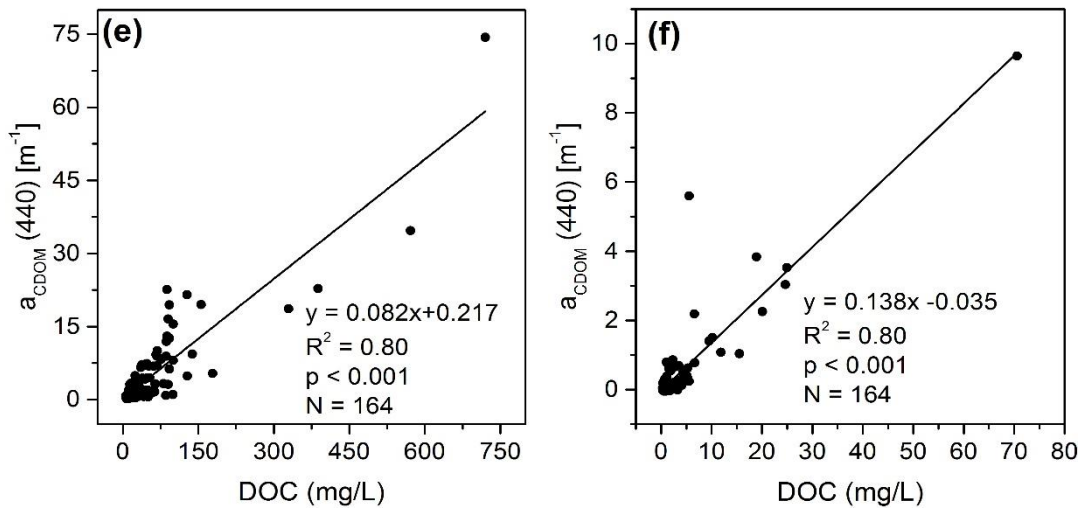
804

805 Fig.6. Relationship between DOC and $a_{CDOM}(440)$ in different types of inland waters,
 806 (a) fresh water lakes, (b) saline water lakes, (c) river and stream waters, (d) urban waters,
 807 (e) ice covered lake underlying waters, and (f) ice melting waters. The regression
 808 metrics without these high DOC concentrations in Fig.6b-f were listed in Tables S6.

809



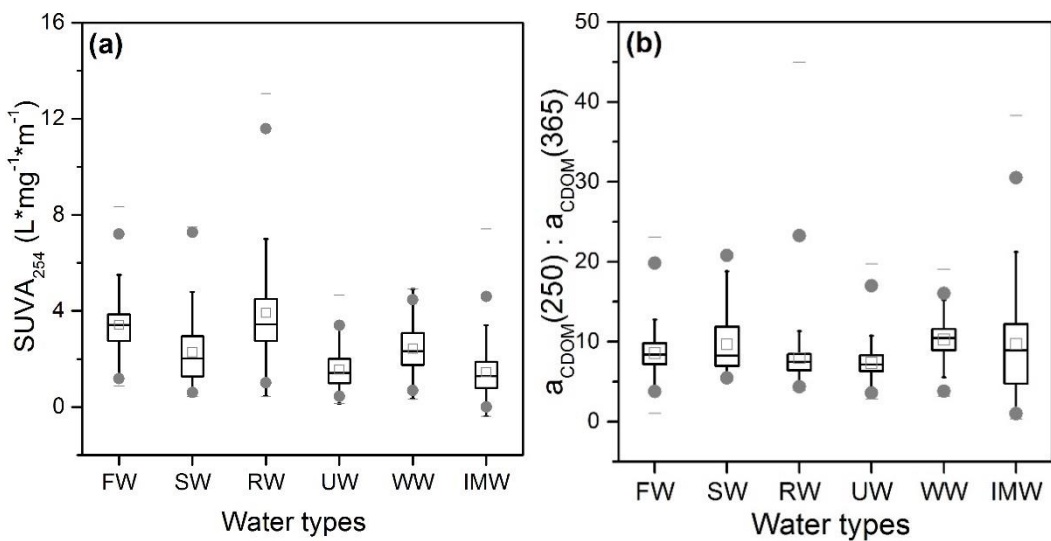
811



812

813

814 Fig.7. Comparison of (a) SUVA₂₅₄, and (b) M values ($a_{CDOM}(250) / a_{CDOM}(365)$) in
 815 various types of inland waters. FW, fresh lake water; SW, saline lake water, RW,
 816 river or stream water; UW, urban water; WW, ice covered waters from Northeast China; IMW,
 817 ice melt waters from Northeast China.



818

819

820

821

822

823

824

825

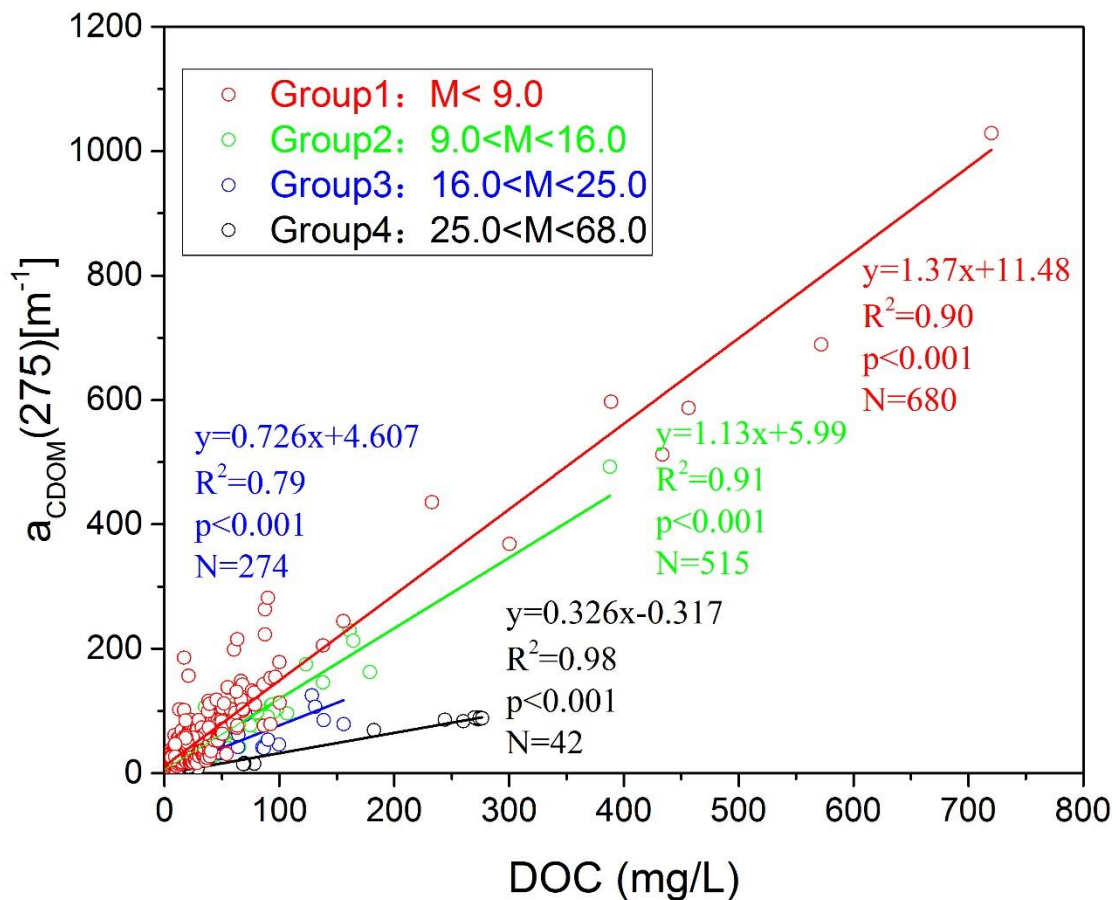
826

827

828

829
830
831
832
833
834
835
836
837
838
839
840
841
842

843 Fig.8. Relationship between DOC and $a_{CDOM}(275)$ sorted by M ($a_{CDOM}(250)/a_{CDOM}(365)$)
844 values, Group 1: $M < 9.0$; Group 2: $9.0 < M < 16.0$; Group 3: $16.0 < M < 25.0$; Group 4:
845 $25.0 < M < 68.0$.



846
847
848
849
850

851

852

853

854

855

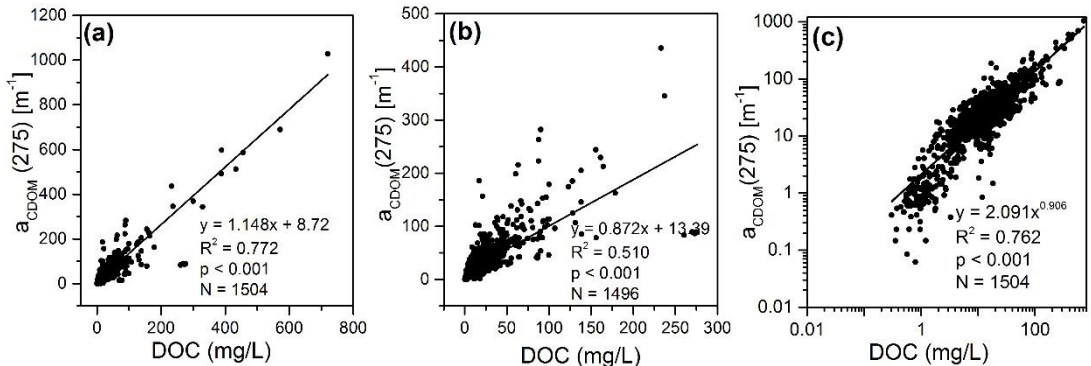
856

857

858

859

860 Fig.9. the relationships between $a_{CDOM}(275)$ and DOC concentrations, (a) regression
861 model with pooled dataset; (b) regression model with DOC concentration less than 300
862 mg/L; (c) regression model with power fitting function based on log-log scale.



863

864

865

866

867

868

869

870

871

872

873

874

875

876

877

878

879 **Tables**

880

881 Table 1. Water quality in different types of waters, DOC, dissolved organic carbon; EC,
 882 electrical conductivity; TP, total phosphorus; TN, total nitrogen; TSM, total suspended
 883 matter; Chl-a, chlorophyll-a concentration.

		DOC (mg/L)	EC μs/cm	pH	TP (mg/L)	TN (mg/L)	TSM (mg/L)	Chl-a (μg/L)
FW	Mean	10.2	434.0	8.2	0.5	1.6	67.8	78.5
	Range	1.9-90.2	72.7-1181.5	6.9-9.3	0.01-10.4	0.001-9.5	0-1615	1.4-338.5
SW	Mean	27.3	4109.4	8.6	0.4	1.4	115.7	9.0
	Range	2.3-300.6	1067-41000	7.1-11.4	0.01-6.3	0.6-11.0	1.4-2188	0-113.7
RW	Mean	8.3	10489.1	7.8-9.5	-	-	-	-
	Range	0.9-90.2	3.7-1000	8.6	-	-	-	-
UW	Mean	19.44	525.4	8.0	3.4	3.5	50.5	38.9
	Range	3.5-123.3	28.6-1525	6.4-9.2	0.03-32.4	0.04-41.9	1-688	1.0-521.1
WW	Mean	67.0	1387.6	8.1	0.7	4.3	181.5	7.3
	Range	7.3-720	139-15080	7.0-9.7	0.1-4.8	0.5-48	9.0-2174	1.0-159.4
IMW	Mean	6.7	242.8	8.3	0.19	1.1	17.4	1.1
	Range	0.3-76.5	1.5-4350	6.7-10	0.02-2.9	0.3-8.6	0.3-254.6	0.28-5.8

884

885 Note: FW, fresh water lake; SW, saline water lake, RW, river or stream water; UW, urban water;
 886 WW, ice covered winter water from Northeast China; IMW, ice melt water from Northeast China.

887

888

889

890

891

892

893

894

895

896

897

898

899

900

901

902

903 Table 2. Descriptive statistics of dissolved organic carbon (DOC) and $\alpha_{CDOM}(440)$ in
 904 various types of waters. Min, minimum; Max, maximum; S.D, standard deviation.
 905

Type	Region	DOC (mg/L)				$\alpha_{CDOM}(440)$ [m^{-1}]			
		Min	Max	Mean	S.D	Min	Max	Mean	S.D
River	Liaohe	3.6	48.2	14.3	9.49	0.46	3.68	0.92	0.58
	Qinghai	1.2	8.5	4.4	1.96	0.13	2.11	0.54	0.63
	Inner Mongolia	16.9	90.2	40.4	24.84	0.32	7.46	1.03	2.11
	Songhua	0.9	21.1	8.1	4.96	0.32	18.93	3.2	4.19
Saline	Qinghai	1.7	130.9	67.9	56.7	0.13	0.86	0.36	0.23
	Hulunbir	8.4	300.6	68.5	69.2	0.82	26.21	4.41	4.45
	Xilinguole	3.74	45.4	14.2	8.8	0.36	4.7	1.34	0.88
	Songnen	3.6	32.6	16.4	7.4	0.46	33.80	2.4	3.78

906
 907
 908
 909
 910
 911
 912
 913
 914
 915
 916
 917
 918
 919
 920
 921
 922
 923
 924
 925
 926
 927
 928
 929
 930

931 Table 3. Fitting equations for DOC against $a_{CDOM}(275)$ in different types of waters
 932 except ice covered lake underlying water and ice melting waters.

Water types	Region or Basin	Equations	R^2	N
Freshwater lakes	Northeast Lake Region	$y = 3.13x - 3.438$	0.87	102
	MengXin Lake Region	$y = 2.16x - 1.279$	0.90	63
	East Lake Region	$y = 1.98x + 7.813$	0.66	69
	Yungui Lake Region	$y = 1.295x - 44.56$	0.71	54
Saline lakes	Songnen Plain	$y = 2.383x + 1.101$	0.92	159
	East Mongolia	$y = 1.791x + 8.560$	0.67	57
	West Mongolia	$y = 1.133x + 3.900$	0.81	46
	Tibetan Lake Region	$y = 0.864x + 2.255$	0.84	83
Rivers or streams	Branch of the Nenjiang River	$y = 7.655x - 42.64$	0.81	33
	Songhua River stem	$y = 3.759x - 6.618$	0.71	29
	Branch of Songhua River	$y = 8.496x - 12.14$	0.98	33
	Liao River Autumn 2012	$y = 1.099x + 3.900$	0.80	38
	Liao River Autumn 2013	$y = 1.073x - 4.157$	0.88	28
	Rivers from North China	$y = 3.154x - 1.207$	0.87	48
	Rivers from East China	$y = 3.037x - 2.585$	0.88	47
	Rivers from Tibetan Plateau	$y = 2.345x + 2.375$	0.87	41
Urban waters	Waters from Changchun	$y = 2.471x - 2.231$	0.54	48
	Waters from Harbin	$y = 1.413x - 4.521$	0.67	31
	Waters from Beijing	$y = 0.874x + 11.12$	0.63	27
	Waters from Tianjin	$y = 0.994x + 7.368$	0.57	23

933

934

935